forests

MDPI

Article

Growth and Multispectral Analysis of New Black Locust (*Robinia pseudoacacia* L.) Clones

Tamás Ábri [1], József Csajbók [2,*], Zsolt Keserű [1], Gergely Szabó [3] and Loránd Szabó [3]

[1] Forest Research Institute, Department of Plantation Forestry, University of Sopron, H-9400 Püspökladány, Hungary
[2] Institute of Crop Production, Breeding and Plant Technology, Faculty of Agriculture, Food Science and Environmental Management, University of Debrecen, H-4032 Debrecen, Hungary
[3] Department of Physical Geography and Geoinformation Systems, Faculty of Science and Technology, University of Debrecen, H-4032 Debrecen, Hungary
* Correspondence: csj@agr.unideb.hu

Abstract

Black locust (*Robinia pseudoacacia* L.) breeding is an important component of plantation forestry in Central and Eastern Europe; however, clone trials are still mainly evaluated using conventional field surveys, and the application of high-resolution red-edge satellite indices at the intraspecific level remains rarely applied. As a result, less information is available on the phenological status of black locust clones derived from red-edge satellite data. This study evaluates a clone trial established in Eastern Hungary on slightly acidic Arenosol soil, assessing the growth performance and seasonal spectral dynamics of newly bred black locust clones during their fifth growing season by integrating field measurements with PlanetScope-derived Normalized Difference Red-Edge Index (NDRE) time series. Clone NK2 exhibited the most vigorous growth, reaching a mean height of 11.1 ± 0.15 m and a diameter at breast height (DBH) of 11.21 ± 0.19 cm, which were 35.4% greater in height and 19.0% larger in DBH than those (8.2 ± 0.12 m height, and 9.42 ± 0.23 cm diameter) of the control ('Üllői' cultivar). Clone PL251 also exceeded the control by 25.6% in height and 19.2% in DBH. Spectral analysis (NDRE value ± standard error) revealed marked differences in phenological development: in the early stage (April 15), NK1 and PL040 had the highest NDRE values (0.472 ± 0.020 and 0.461 ± 0.019), whereas NK2 showed delayed leaf emergence (0.398 ± 0.019). By June 21, PL251 had reached an NDRE value of 0.692 ± 0.013, which was higher than that of the control (0.673 ± 0.016). In mid-July, NDRE peaked for NK2 and NK1 (0.732 ± 0.012 and 0.731 ± 0.013), with 'Üllői' showing consistently lower values across the season. In the final stage, NK2 maintained the highest NDRE values (October 22: 0.618 ± 0.015; November 9: 0.466 ± 0.021), indicating prolonged photosynthetic activity, while NK1 and 'Üllői' declined earlier (e.g., November 9: 0.354 ± 0.018 and 0.390 ± 0.027, respectively). These findings highlight NK2 and PL251 as superior candidates for high-yield, climate-resilient tree plantations because of their strong growth and extended physiological activity.

Keywords: PlanetScope; spectral index; NDRE; black locust improvement

Academic Editor: Aleksandar Dj Valjarević

Received: 20 January 2026
Revised: 30 January 2026
Accepted: 3 February 2026
Published: 4 February 2026

1. Introduction

The black locust (*Robinia pseudoacacia* L.) is a fast-growing, nitrogen-fixing tree species native to North America, but it has been widely introduced and cultivated across temperate regions of the world, including Europe and Asia [1]. Due to its rapid growth, high

adaptability to diverse site conditions, and hard and durable wood, as well as valuable nectar production, it is considered an important multifunctional tree species in many countries [2]. Black locust is used for a variety of purposes globally, such as biomass energy production [3,4], timber [2,5], erosion control [6], reclamation of degraded lands [7,8], and apiculture [9,10]. In Central and Eastern Europe, particularly in Hungary, it is one of the most commonly planted exotic tree species, owing to its above-mentioned ecological and economic benefits [2,5].

Despite these advantages, black locust cultivation also faces challenges related to silvicultural and technological traits, such as crooked and/or forked stem, low industrial wood yield, and susceptibility to frost. These issues have prompted long-term breeding programs in several countries aimed at improving stem form, increasing tree volume and nectar yield, and enhancing drought tolerance [2,9,11].

As a result of more than 60 years of black locust improvement research in Hungary, numerous cultivars have been bred, and several new clones are currently under continuous testing [11]. In addition to growth in height and diameter, the studies also cover the phytophysiological traits (photosynthetic activity, transpiration, water use efficiency) [12] and tree health of the clones [13]. This can be assisted by various vegetation indices.

Vegetation indices (VIs) are essential tools for monitoring plant health and growth dynamics by analyzing spectral reflectance across the visible electromagnetic spectrum, Near-Infrared (NIR), and shortwave infrared (SWIR) spectral ranges [14]. These indices enable the detection of physiological stress, phenological changes, and ecosystem degradation, supporting informed interventions in agriculture and forestry [15–23]. Among these, the Normalized Difference Red-Edge Index (NDRE) is particularly effective due to its use of the red-edge (RE) band, which is more sensitive to chlorophyll variations and less prone to saturation at high biomass levels than the NDVI. Since NDRE, as an indirect indicator, effectively reflects photosynthetic capacity and canopy density, it serves as a robust proxy for long-term biomass accumulation [24,25].

Observing vegetation requires high spectral, spatial and temporal resolutions from different satellite sensors. Relevant existing studies operate with freely available satellite images, e.g., Sentinel-2 and Landsat, but PlanetScope images [26] have not been applied before for black locust observation. Landsat satellites even do not have RE bands and their coarser spatial resolution (30 m) also does not make them suitable for investigating small parcels. Although Sentinel-2 satellites have 10 m spatial resolution, their RE bands only have a 20 m spatial resolution, which is also not suitable for smaller parcels. Thus, this is the first study integrating high-resolution PlanetScope NDRE data to assess the phenological divergence between black locust clones in Europe. The PlanetScope constellation provides approximately 200 multispectral satellites with a spatial resolution of 3 m and a daily revisit time. The latest SuperDove satellites of the constellation operates with eight spectral bands, including the RE spectral band next to the regular Blue, Green, Red and Near-Infrared bands, which makes it capable of calculating the NDRE index [26], and it also means more than 40 times more data compared to the spatial resolution of the Sentinel-2 satellites.

This study aimed to compare growth and phenological trends of new black locust clones (PL251, NK1, PL040, NK2) and the state-approved cultivar 'Üllői' during the 2024 vegetation period by answering the following major questions:

1. Do the studied black locust clones exceed the growth parameters (height and diameter) of the state-approved 'Üllői' cultivar (control)?
2. Is there any difference in the observed spectral index values between the studied clones during the vegetation period of 2024?

2. Materials and Methods

2.1. Site Characteristics

The clone trial was set up in spring 2020 at the site of Napkori Erdőgazdák Ltd., Eastern Hungary (UTM 563,167 E; 5,307,770 N) (Figure 1). In this experimental plantation, four new clones and one state-approved cultivar were compared. The set up was in a block design, with 14 rows per block for each clone, planted in a 2.5 × 2.5 m pattern. The total length of the experiment was 270 m and the total width was 35 m. For the NDRE values, we took into account values ranging from 97 to 220 pixels per block. The site has humous sandy soil; in the World Reference Base for Soil Resources, it is Arenosol [12].

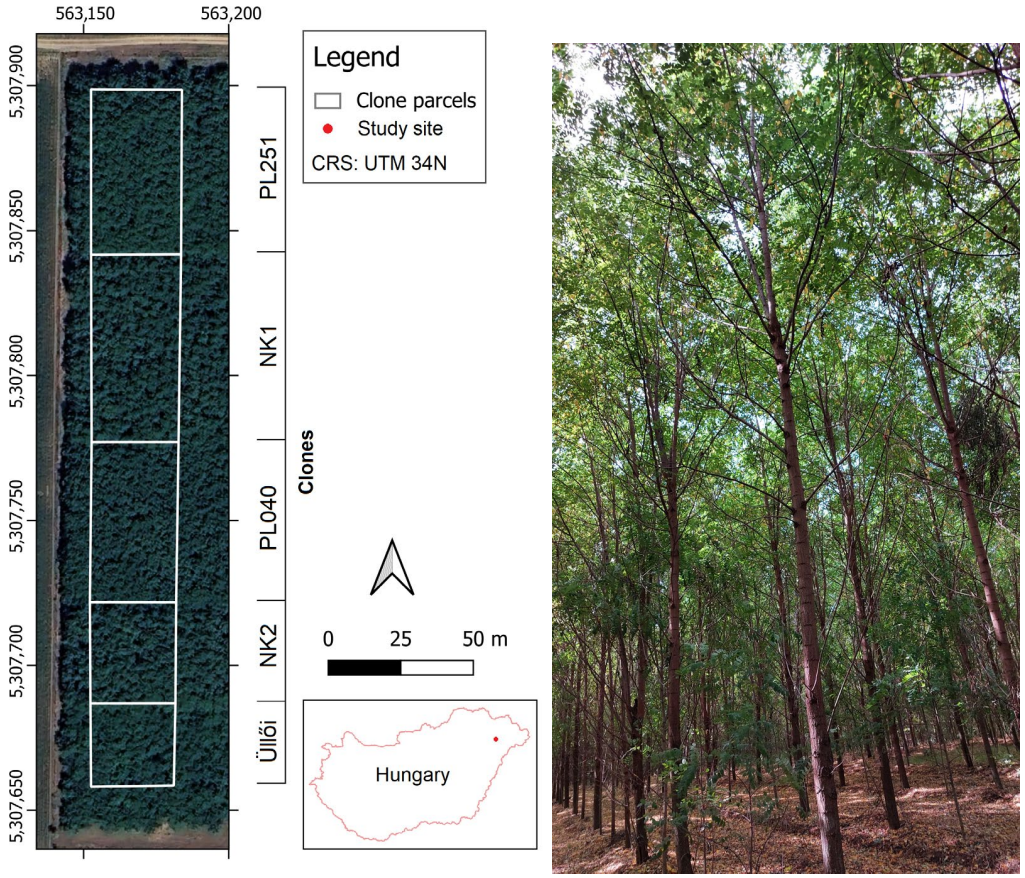

Figure 1. Location of the clone trial and the photograph of clone PL251.

The humus content is very low (Hu% < 1). The soil plasticity index (K_A) is 28. The acidity of the upper soil layers (0–160 cm) is acidic (pH_{KCl} = 4.4–5.0), but in the layer, from 160 to 200 cm, it is slightly alkaline (pH_{KCl} = 7.4). The nutrient status of the soil is very low (N% < 0.05; AL-P_2O_5: 0.65–9.68 mg per 100 g; AL-K_2O: 5.49–29.59 mg per 100 g).

A meteorological station is located a few kilometers from the clone trial, which is part of the national network [27]. The data show an average annual temperature of 11.2 °C years and an average precipitation of 549.7 mm, over 20-year period. The meteorological data for the period 2005–2024, including 2024, are analyzed in detail in the Section 3. The precipitation was segmented into 5-year periods, based on which the monthly precipitation totals for 2005–2009; 2010–2014; 2015–2020; and 2020–2024 were analyzed separately.

2.2. Tree Growth Measurements

We measured the height and diameter (at breast height) of the trees (30 stems per clones on 27 January 2025). We used a NIKON Forestry Pro II laser rangefinder (Nikon

Corp., Tokyo, Japan) for height measurements and a HAGLÖF Mantax Precision Blue caliper (500 mm) (Haglöf AB, Långsele, Sweden) for diameter measurements.

2.3. Multispectral Analysis with Satellite Imagery

In this study, we employed the NDRE spectral index [28] during the multispectral satellite analysis. Compared to indices such as NDVI, NDRE provides a more accurate assessment of the overall physiological status of vegetation due to its sensitivity to the RE spectral band. Moreover, NDRE does not exhibit saturation effects in areas with dense canopies or lush vegetation, which is a known limitation of NDVI [28].

$$\mathrm{NDRE} = (\mathrm{NIR} - \mathrm{RE})/(\mathrm{NIR} + \mathrm{RE}), \quad (1)$$

where NIR (Near-Infrared) represents the surface reflectance values from Band 8 of the PlanetScope SuperDove sensor, and RE (Red Edge) represents the surface reflectance values from Band 7 of the PlanetScope SuperDove sensor.

We analyzed the NDRE values of the vegetation stands over the period from 15th April to 9 November 2024, encompassing the full growing season of the black locust clones. We ordered 14 cloud-free PlanetScope SuperDove (Planet Labs PBC, San Francisco, CA, USA) satellite images with 3 m spatial resolution from the Planet Explorer website [29]. The pixel values (n = 97–220, varied by parcels) of images were calibrated to surface reflectance during the data preparation at the Planet's side; this provided the comparability of images taken on different dates. To mitigate edge effects, only those pixels whose centroids fell within the predefined boundaries of each plot were included in the analysis. Precise plot boundaries were available and utilized to ensure spatial accuracy. First, the NDRE indices were calculated for all the images using QGIS 3.40.4 [30] by applying the NDRE formula (Equation (1)). At each date, we calculated and examined the mean NDRE values for each clone by applying a Python (ver. 3.13) code [31] to extract all the NDRE index pixel data within each clone parcel for each image and then calculated the mean values from the extracted data.

2.4. Statistical Analyses

Before comparing the clones, the homogeneity of variances was tested using Levene's test, and the normal distributions in the groups were tested using the Shapiro–Wilk test. As the measured height and diameter data met the parametric test conditions, we used one-way ANOVA and Tukey's post hoc test for pairwise comparison. We would like to point out that NDRE pixel values originate from the same area and have common environmental conditions; therefore, they cannot be considered as completely independent statistical units. Consequently, our NDRE analyses focused on consistent temporal patterns and the magnitude of differences rather than formal hypothesis testing. Statistical analyses were performed with IBM SPSS 25.0 (IBM Corp., Chicago, IL, USA) statistical software.

3. Results

3.1. Climate Conditions

The negative impacts of local climate change (e.g., drought, uneven precipitation distribution, and elevated temperatures) are increasingly evident near the settlement of Napkor. Over the past 20 years, average temperatures have shown an increasing trend. In the studied period, 2024 recorded the highest annual average temperature at 12.9 °C, which exceeded the long-term average (11.2 °C) by 15% (Figure 2).

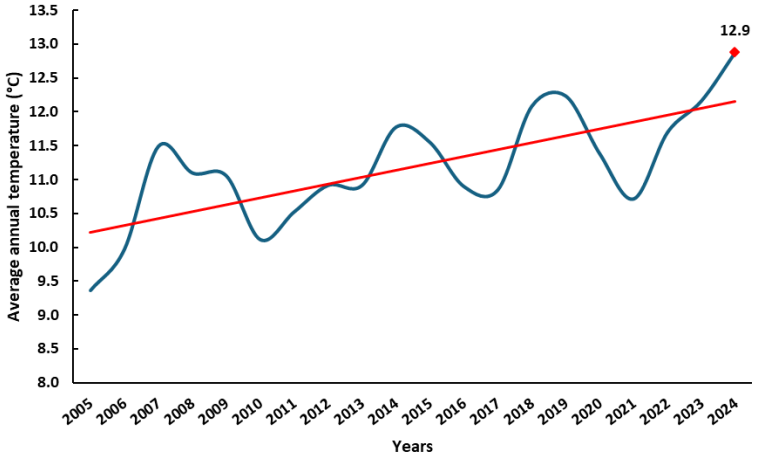

Figure 2. Trend of increasing annual average temperatures (°C) near Napkor, Hungary (2005–2024), with a 2024 record high. Data recorded at the HungaroMet Ltd. meteorological station in Napkor, Hungary. Red line: linear regression function (Y = 0.1015x + 10.119); blue line: average annual temperature.

Precipitation distribution was analyzed in 5-year cycles (Figure 3), allowing clearer trends to emerge: a decline in spring precipitation, an increase in winter precipitation (December–February), and growing irregularity in rainfall distribution. Based on the average monthly values over the last five years (2020–2024), the total spring (March–May) precipitation was 95 mm—46 mm (48%) less than in the 2005–2009 period. Compared to 2010–2014, this represents a 44% decrease, and compared to 2015–2019, a 31% decrease. During the primary growing season of trees (May–August), precipitation also showed a declining trend. While the average for this period was 268 mm between 2005 and 2009, it dropped by 20% to 223 mm in 2020–2024.

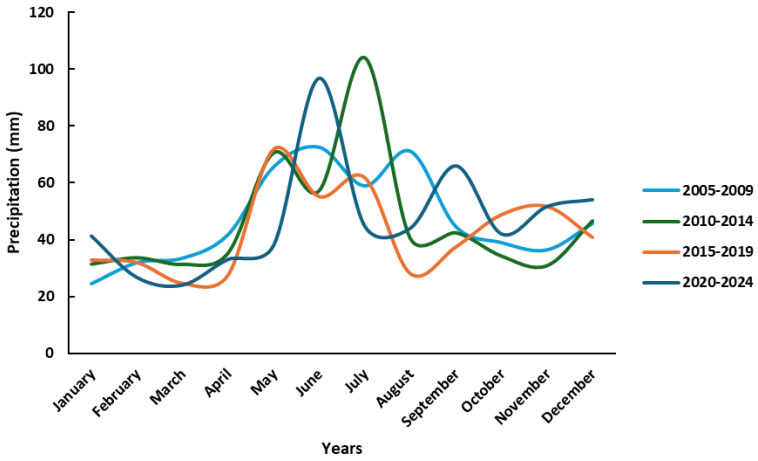

Figure 3. Temporal variability of monthly precipitation (mm) in 5-year periods near Napkor, Hungary (2005–2024). Data recorded at the HungaroMet Ltd. meteorological station in Napkor, Hungary.

Precipitation distribution has also become more uneven, as reflected in the standard deviation of monthly precipitation for each period: 16 (2005–2009), 21.8 (2010–2014), 15.1 (2015–2019), and 19.5 (2020–2024). This trend was even more pronounced for the May–August period, with the lowest variability observed in 2005–2009 (6.1), and the highest in 2020–2024 (27.4). The standard deviation for 2010–2014 and 2015–2019 were 20 and 18.7, respectively.

A notable increase in winter precipitation was also observed. Between 2005 and 2009, the total for December to February was 103 mm, compared to 122 mm in the 2020–2024 period—an 18% increase.

In 2024, total annual precipitation was 506 mm, which is 9% lower than the 20-year average (550 mm). The monthly precipitation and average monthly temperatures for 2024 are illustrated in Figure 4. Except for January, April, June, September, and October, monthly precipitation was significantly below the long-term monthly averages. Monthly mean temperatures exceeded the 2005–2024 monthly averages for most of the year. Particularly noteworthy are the exceptionally warm months of February (8.2 °C) and March (9.7 °C), as well as July (24.3 °C) and August (23.8 °C). Compared to long-term averages, mean monthly temperatures were higher by 6.5 °C in February, 3.4 °C in March, 2.3 °C in July, and 2.1 °C in August.

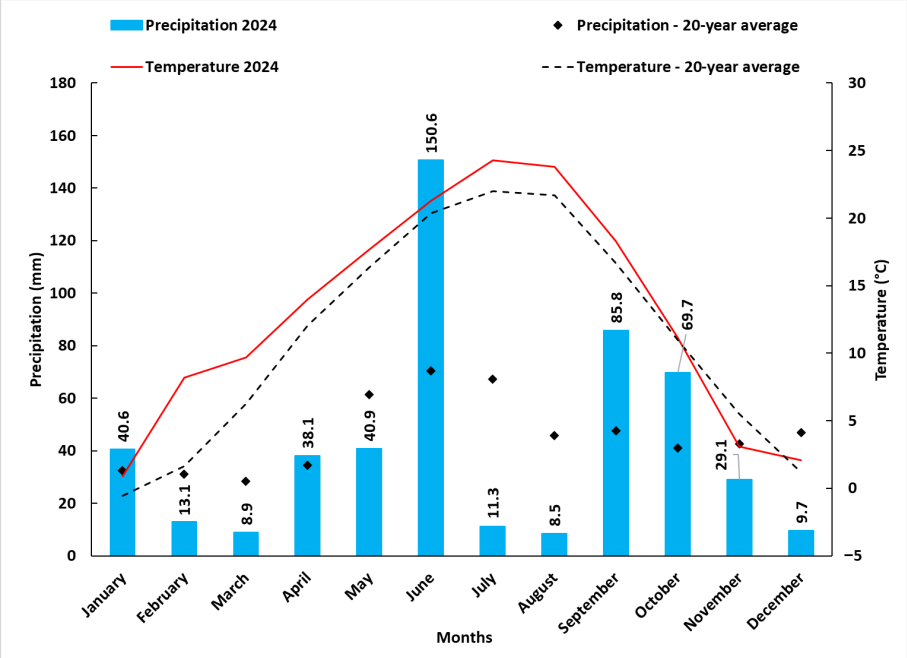

Figure 4. Monthly precipitation totals and temperature averages in Napkor, Hungary (2024) compared to 20-year means. Numbers above the bars indicate monthly precipitation sums for 2024. Data recorded at the HungaroMet Ltd. meteorological station in Napkor, Hungary.

This data clearly illustrate the changing climatic conditions, which significantly complicate forest cultivation efforts.

3.2. Height and Diameter Growth

The clones planted in 2020 demonstrated rapid juvenile growth. By early 2025, at five years of age, the trees reached heights of 8–11 m and DBH values of 8–11 cm. There were significant differences ($p = 0.05$) in the mean (± standard error) height and diameter between the clones. All tested clones outperformed the control 'Üllői' black locust in both height (8.2 ± 0.12 m) and diameter (9.42 ± 0.23 cm). According to Tukey's test, NK2 was the best performer, with a height of 11.1 ± 0.15 m and diameter of 11.21 ± 0.19 cm. In terms of height, NK2 was significantly better than the other clones. There were no statistically significant differences between NK1 (10.0 ± 0.12 m), PL040 (10.3 ± 0.12 m), and PL251 (10.3 ± 0.08 m) heights. For DBH, no significant differences were found between NK2, PL251 (11.23 ± 0.18 cm), and NK1 (10.68 ± 0.21 cm), nor between NK1 and PL040 (10.26 ± 0.15 cm). However, NK2 and PL251 differed significantly from PL040 (Figure 5).

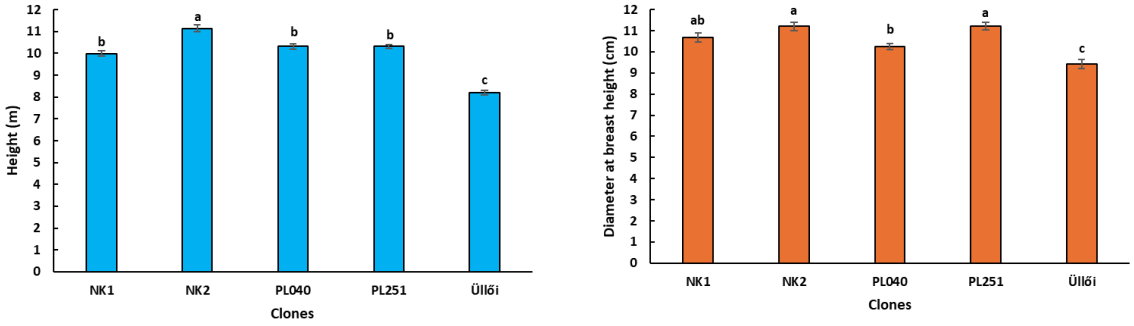

Figure 5. Height (**a**) and diameter (at breast height) (**b**) of black locust clones (27 January 2025), results of one-way ANOVA (Tukey's test); ±standard error; the different letters mean significant difference at $p = 0.05$ among the clones.

3.3. Multispectral Analysis

The results of the multispectral analysis are shown in Figure 6. NDRE values are presented for the period from April 15 to 9 November 2024. The lowest NDRE values (0.40–0.47) were observed at the beginning (April 15) and end (November 9; 0.35–0.47) of the vegetation period. A steady increase was recorded from April to mid-July, peaking on July 18 (0.71–0.73). High NDRE values persisted until the second half of September, followed by a notable decline (0.65–0.69) thereafter. By October, the values dropped to 0.57–0.62, with a further decrease at the beginning of November.

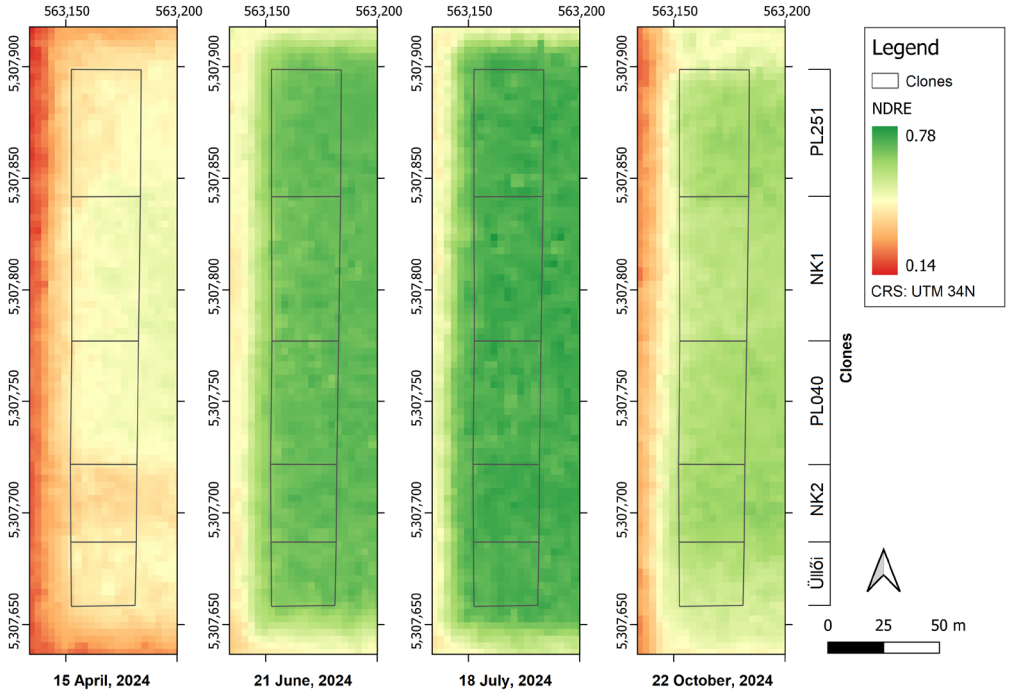

Figure 6. NDRE indices of the clones at four selected dates.

The temporal patterns of clones were compared based on their average (±standard deviation) NDRE values (Figure 7). In the early stage (April 15–May 29), NK1 and PL040 had the highest NDRE values, whereas NK2 had the lowest. On April 15, NDRE values were 0.472 (±0.020) for NK1 and 0.461 (±0.019) for PL040, respectively. In contrast, the values for PL251 (0.438 ± 0.020), 'Üllői' control (0.426 ± 0.015), and NK2 (0.398 ± 0.019) were markedly lower. Each clone was different from the others on this date, indicating

variation in leaf emergence timing. Clones NK1 and PL040 showed elevated NDRE values compared to the control; the differences were 11% and 8%, respectively.

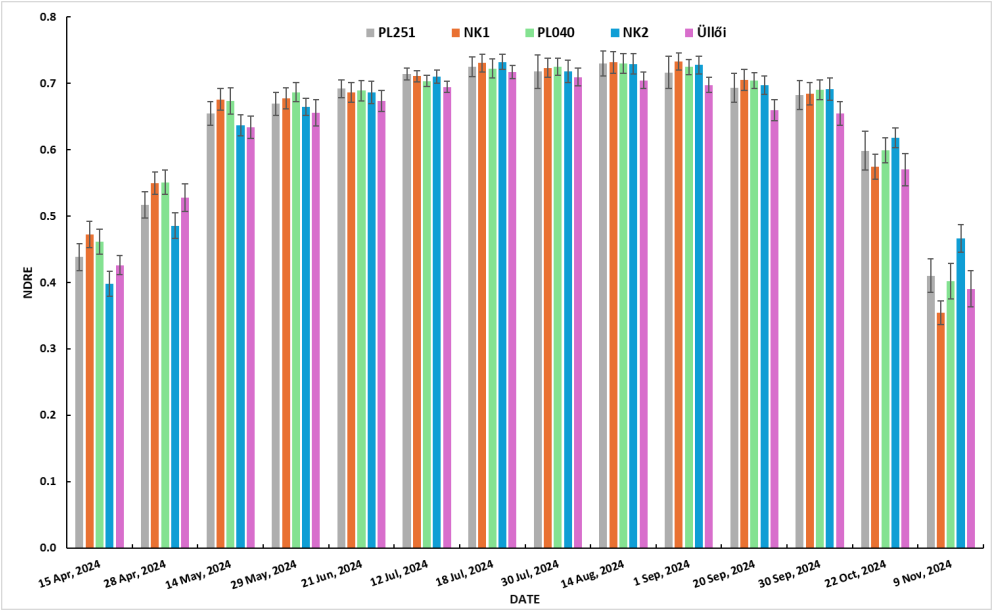

Figure 7. NDRE indices (mean ± standard deviation) of black locust clones (from 15 April to 9 November 2024).

At the first summer date (June 21), PL251 and PL040 performed best with values of 0.692 (±0.013) and 0.689 (±0.016), respectively, with negligible difference between them. PL251 outperformed NK1, NK2, and 'Üllői', while PL040 only slightly exceeded NK1 (0.687 ± 0.015) and NK2 (0.686 ± 0.017). The 'Üllői' control had a lower value (0.673 ± 0.016) than that of all clones, which was approximately 2–3% lower than that of the other clones. From this point until October 22, the 'Üllői' clone consistently displayed the lowest NDRE values.

In mid-July (18 July), when the clones reached peak NDRE values, NK1 (0.731 ± 0.013) and NK2 (0.732 ± 0.012) were the top performers, with no difference between them, but differences from the other clones. PL251 (0.725 ± 0.015) and PL040 (0.723 ± 0.014) also did not differ from each other. The control Üllői had a lower NDRE value (0.717 ± 0.010). In this period the studied clones exceeded the control by 1–2%.

By September 20, the NDRE values began to decline. NK1 (0.705 ± 0.016) and PL040 (0.705 ± 0.012) had the highest values, which were markedly different from the other clones, though not from each other. PL251 (0.693 ± 0.022) and NK2 (0.697 ± 0.014) were nearly similar to each other. The 'Üllői' cultivar again had the lowest value (0.660 ± 0.016), 4–6% below the values observed in the other clones.

In the final months, clone NK2, which initially showed the lowest value, proved to be the best performer (October 22: 0.618 ± 0.015; November 9: 0.466 ± 0.021), exceeding the control by 20% on November 9, and demonstrating a strong mid-to-late-season vigor. The lowest values in both months were recorded for NK1 (October 22: 0.575 ± 0.019; November 9: 0.354 ± 0.018) and 'Üllői' (October 22: 0.570 ± 0.024; November 9: 0.390 ± 0.027).

It should be noted that, throughout the entire growing season, the NDRE values of clone PL040 consistently exceeded those of the control, with the difference ranging between 1% and 8%.

Overall, the NDRE time-series analysis demonstrates distinct clone-specific patterns in seasonal canopy development and spectral performance, supporting the differenti-

ation of clones based on remotely sensed indicators of vitality and photosynthetically active biomass.

4. Discussion

Understanding clonal differences in growth dynamics and seasonal physiological activity is essential for improving plantation forestry under increasingly variable climatic conditions. Integrating field-based growth measurements with remote-sensing indicators provides an opportunity to evaluate both the structural development and temporal patterns of canopy activity in a non-destructive manner.

Consistent with previous studies [12,32], in the fifth growing season, the NK2 and PL251 clones proved to be the best performers in terms of height and diameter, while the 'Üllői' cultivar exhibited the weakest growth. 'Üllői' was significantly outperformed by the newly tested clones in terms of both height and diameter. Moreover, the height of 10–11 m and diameter of 10–11 cm significantly exceeded the corresponding values published in several growth and yield tables developed for black locust stands [33]. According to a review [2], black locust can exhibit rapid growth under favorable site conditions (i.e., soils rich in humus and nutrients, well-aerated, and with good water balance), reaching a height of 10 m by the age of five.

Temporal variation in NDRE values revealed clear phenological differences between the studied clones. At the beginning of the growing season (April–May), all clones exhibited low NDRE values, indicating an early leaf-flushing phase. PL251 and NK1 showed the highest NDRE values during the early and mid-growing seasons (June–July), suggesting higher chlorophyll content, which may be associated with enhanced photosynthetic activity at the canopy level [34,35]. In contrast, the NK2 clone—despite its superior growth performance—initially exhibited low NDRE values, which likely indicate delayed leaf flushing. However, from mid-July onward, it became one of the clones with the highest NDRE values. This trend is supported by earlier measurements showing that NK2 produced the best values in terms of photosynthetic activity [12,36]. On the other hand, the 'Üllői' cultivar consistently showed significantly lower NDRE values throughout almost the entire vegetation period compared to the other clones, possibly indicating different physiological traits or lower stress tolerance. During autumn (September–November), the NDRE values of all clones gradually declined, reflecting the natural process of senescence and decreasing chlorophyll content. In October and November, despite its late leaf-out, the NK2 clone performed the best, whereas NK1, which had shown excellent values in the early phases, had the lowest NDRE values. Besides NK2, the other high-performing clone, PL251, maintained relatively high NDRE values in the final months. However, clone PL040 consistently showed higher NDRE throughout the growing period compared to the control, which suggests that PL040 maintains a stable canopy structure and chlorophyll-related spectral response across phenological stages. As NDRE reflects changes in chlorophyll content, it is thus an indirect indicator of physiological traits such as photosynthesis and overall tree vitality. These results suggest that photosynthetic activity may be higher and more prolonged in these three clones than in the others.

The primary objective of working with these black locust clones is to meet the increasing demand for high-quality timber from industrial plantations established with such genetic material [12]. Beyond this, their environmental utility, particularly their carbon sequestration potential, is of great importance. The carbon sequestration capacity of black locust stands increases with age, highlighting their vital role in environmental management, especially in semi-arid regions [37].

Remote-sensing-based vegetation index analysis of forests and tree plantations has made substantial progress in recent decades, particularly using Sentinel-2 and

Landsat-8 satellite data [38–40]. However, in the case of clone trials with small parcels, PlanetScope would be more suitable, because it ensures denser temporal coverage, and compared to the spatial resolution of the Sentinel 2 satellites, it provides more than 40 times more data. There are indeed several well-known limiting factors, such as soil background, shading, and canopy structure; nevertheless, differences between the clones can still be detected in their early phenological stages. While cloud coverage remains a limiting factor for all optical remote-sensing data sources, PlanetScope's daily revisit time increases the number of potential cloud-free acquisitions. Moreover, unlike Landsat sensors, PlanetScope includes a RE band, enabling improved sensitivity to variations in canopy chlorophyll content [26,41,42]. In the context of monitoring stand development, vegetation indices—especially NDVI and NDRE—play a crucial role in assessing plant health and biological activity [43]. Although NDVI is widely used, it tends to saturate quickly in dense canopies. In contrast, NDRE is more sensitive to chlorophyll content variations and less prone to saturation, making it more suitable for evaluating more developed vegetation [22–24].

The findings of this study are particularly relevant for plantation forestry in Central and Eastern Europe, where black locusts are widely planted on sandy, drought-prone soils with limited nutrient availability. Clones combining rapid juvenile growth with extended seasonal canopy activity, such as NK2, PL251 and PL040, may offer improved productivity and resilience under climates characterized by higher temperatures and increasingly uneven precipitation patterns.

According to a recent FAO (2024) report [44] on the state of the world's forests, global wood demand is projected to rise significantly by 2050. In response, the area of forest plantations may need to expand by 20 to 40 million hectares in the coming years. Meeting this demand will require innovative biotechnologies. Ongoing research in genetics and tree breeding aims to enhance productivity, disease resistance, and the ability of trees to cope with the adverse impacts of climate change [45–47]. In this context, evaluating the growth and physiological performance (e.g., photosynthetic activity) of tree species such as black locust is pivotal. As a versatile species, black locust is expected to play a key role in future forest management strategies, particularly in plantation forestry.

5. Conclusions

This study demonstrated that newly bred black locust clones exhibit substantial differences in both growth performance and seasonal canopy dynamics. In their fifth growing season, clones NK2 and PL251 exceeded the state-approved 'Üllői' cultivar by up to 25–35% in height and approximately 19% in DBH, confirming their superior juvenile growth potential. The NDRE time series derived from high-resolution PlanetScope imagery revealed distinct phenological patterns between clones, particularly in early leaf-out and delayed canopy senescence.

The results indicate that the integration of field measurements with red-edge-based satellite indices provides a robust framework for evaluating clonal performance. In practice, this approach can support forest managers and state forestry organizations in monitoring plantation performance, breeding programs and research institutions in early selection of superior clones, and policy makers and land-use planners in designing afforestation and biomass production strategies under changing climatic conditions. For Central and Eastern Europe, where black locust plays a key role in afforestation and biomass production on marginal sites, NDRE derived from PlanetScope imagery offers a valuable, scalable tool for data-driven decision-making in adaptive forest management. Integrating advanced remote-sensing technologies with conventional forestry practices represents a promising approach to enhance forest management. This synergy supports both economic develop-

ment and ecological sustainability, especially in the context of climate change and land restoration challenges.

Author Contributions: Conceptualization, T.Á. and L.S.; methodology, T.Á. and L.S.; software, G.S. and L.S.; validation, T.Á., J.C., Z.K. and L.S.; formal analysis, L.S.; investigation, T.Á., G.S., J.C. and L.S.; resources, G.S. and L.S.; data curation, T.Á., L.S. and J.C.; writing—original draft preparation, T.Á. and L.S.; writing—review and editing, T.Á.; visualization, T.Á. and L.S.; supervision, T.Á., G.S. and J.C.; project administration, J.C.; funding acquisition, T.Á. and Z.K. All authors have read and agreed to the published version of the manuscript.

Funding: This article was made in the frame of the project TKP2021-NKTA-43, which has been implemented with the support provided by the Ministry of Culture and Innovation of Hungary from the National Research, Development and Innovation Fund, financed under the TKP2021-NKTA funding scheme. The research was further supported by the National Research, Development and Innovation Office (NKFI Office) under grants NKFI K 138079 and NKFI ADVANCED 152950.

Data Availability Statement: Dataset available on request from the authors.

Acknowledgments: The authors express their gratitude to the local forest company (Napkori Erdőgazdák Ltd.) for their valuable support in the fields. In addition, our colleagues are thanked for their help with the fieldwork and assistance.

Conflicts of Interest: The authors declare no conflicts of interest.

Abbreviations

The following abbreviations are used in this manuscript:

NDRE	Normalized Difference Red-Edge Index
NIR	Near-Infrared band
RE	Red-edge band

References

1. Cierjacks, A.; Kowarik, I.; Joshi, J.; Hempel, S.; Ristow, M.; von der Lippe, M.; Weber, E. Biological flora of the British Isles: *Robinia pseudoacacia*. *J. Ecol.* **2013**, *101*, 1623–1640. [CrossRef]
2. Nicolescu, V.N.; Rédei, K.; Mason, W.L.; Vor, T.; Pöetzelsberger, E.; Bastien, J.-C.; Brus, R.; Benčať, T.; Đodan, M.; Cvjetkovic, B.; et al. Ecology, growth and management of black locust (*Robinia pseudoacacia* L.), a non-native species integrated into European forests. *J. For. Res.* **2020**, *31*, 1081–1101. [CrossRef]
3. Manzone, M.; Bergante, S.; Facciotto, G. Energy and economic sustainability of woodchip production by black locust (*Robinia pseudoacacia* L.) plantations in Italy. *Fuel* **2015**, *20*, 555–560. [CrossRef]
4. Zhang, J. Planting black locust (*Robinia pseudoacacia*) forest as a biomass energy resource. In *Coastal Saline Soil Rehabilitation and Utilization Based on Forestry Approaches in China*; Springer: Berlin/Heidelberg, Germany, 2014. [CrossRef]
5. Rédei, K. Management of black Locust (*Robinia pseudoacacia* L.) stands in Hungary. *J. For. Res.* **2002**, *13*, 260–264. [CrossRef]
6. Wang, B.; Liu, G.; Xue, S. Effect of black locust (*Robinia pseudoacacia*) on soil chemical and microbiological properties in the eroded hilly area of China's Loess Plateau. *Environ. Earth Sci.* **2012**, *65*, 597–607. [CrossRef]
7. Woś, B.; Pająk, M.; Krzaklewski, W.; Pietrzykowski, M. Verifying the utility of black locust (*Robinia pseudoacacia* L.) in the reclamation of a lignite combustion waste disposal site in Central European conditions. *Forests* **2020**, *11*, 877. [CrossRef]
8. Kanzler, M.; Böhm, C.; Freese, D. The development of soil organic carbon under young black locust (*Robinia pseudoacacia* L.) trees at a post-mining landscape in eastern Germany. *New For.* **2021**, *52*, 47–68. [CrossRef]
9. Keresztesi, B. *Black Locust*; Akadémia Kiadó: Budapest, Hungary, 1988.
10. Alilla, R.; De Natale, F.; Epifani, C.; Parisse, B.; Cola, G. The flowering of black locust (*Robinia pseudoacacia* L.) in Italy: A phenology modeling approach. *Agronomy* **2022**, *12*, 1623. [CrossRef]
11. Ábri, T.; Cseke, K.; Keserű, Z.; Porcsin, A.; Szabó, F.M.; Rédei, K. Breeding and improvement of black locust (*Robinia pseudoacacia* L.) with a special focus on Hungary: A review. *iForest* **2023**, *16*, 290–298. [CrossRef]
12. Ábri, T.; Keserű, Z.; Borovics, A.; Rédei, K.; Csajbók, J. Comparison of juvenile, drought tolerant black locust (*Robinia pseudoacacia* L.) clones with regard to plant physiology and growth characteristics in Eastern Hungary: Early evaluation. *Forests* **2022**, *13*, 292. [CrossRef]

13. Ábri, T.; Keserű, Z.; Koltay, A. Tree health survey results of juvenile black locust clones. *Acta Silv. Lignaria Hung.* **2024**, *20*, 95–108. [CrossRef]
14. Xue, J.; Su, B. Significant remote sensing vegetation indices: A review of developments and applications. *J. Sens.* **2017**, *2017*, 1353691. [CrossRef]
15. Hawryło, P.; Bednarz, B.; Wężyk, P.; Szostak, M. Estimating defoliation of Scots pine stands using machine learning methods and vegetation indices of Sentinel-2. *Eur. J. Remote Sens.* **2018**, *51*, 194–204. [CrossRef]
16. Lastovicka, J.; Svec, P.; Paluba, D.; Kobliuk, N.; Svoboda, J.; Hladky, R.; Stych, P. Sentinel-2 data in an evaluation of the impact of the disturbances on forest vegetation. *Remote Sens.* **2020**, *12*, 1914. [CrossRef]
17. Galieni, A.; D'Ascenzo, N.; Stagnari, F.; Pagnani, G.; Xie, Q.; Pisante, M. Past and future of plant stress detection: An overview from remote sensing to positron emission tomography. *Front. Plant Sci.* **2021**, *11*, 609155. [CrossRef] [PubMed]
18. Zeng, L.; Wardlow, B.D.; Xiang, D.; Hu, S.; Li, D. A review of vegetation phenological metrics extraction using time-series, multispectral satellite data. *Remote Sens. Environ.* **2020**, *237*, 111511. [CrossRef]
19. Wang, C.; Yang, Y.; Yin, G.; Xie, Q.; Xu, B.; Verger, A.; Descals, A.; Filella, I.; Peñuelas, J. Divergence in autumn phenology extracted from different satellite proxies reveals the timetable of leaf senescence over deciduous forests. *Geophys. Res. Lett.* **2024**, *51*, e2023GL107346. [CrossRef]
20. Grabska-Szwagrzyk, E.; Tymińska-Czabańska, L. Sentinel-2 time series: A promising tool in monitoring temperate species spring phenology. *Forestry* **2024**, *97*, 267–281. [CrossRef]
21. Eitel, J.U.; Vierling, L.A.; Litvak, M.E.; Long, D.S.; Schulthess, U.; Ager, A.A.; Krofcheck, D.J.; Stoscheck, L. Broadband, red-edge information from satellites improves early stress detection in a New Mexico conifer woodland. *Remote Sens. Environ.* **2011**, *115*, 3640–3646. [CrossRef]
22. Marx, A.; Kleinschmit, B. Sensitivity analysis of RapidEye spectral bands and derived vegetation indices for insect defoliation detection in pure Scots pine stands. *iForest* **2017**, *10*, 659. [CrossRef]
23. Bałazy, R.; Hycza, T.; Kamińska, A.; Osińska-Skotak, K. Factors affecting the health condition of spruce forests in Central European Mountains—Study based on multitemporal RapidEye satellite images. *Forests* **2019**, *10*, 943. [CrossRef]
24. Boiarskii, B.; Hasegawa, H. Comparison of NDVI and NDRE indices to detect differences in vegetation and chlorophyll content. *J. Mech. Contin. Math. Sci.* **2019**, *4*, 20–29. [CrossRef]
25. Boiarskii, B.; Sinegovskii, M. Application of NDVI and NDRE vegetation indices in the assessment of soybean productivity under nitrogen controlled-release fertilizer. In Proceedings of the 2022 VIII International Conference on Information Technology and Nanotechnology (ITNT), Samara, Russia, 23–27 May 2022. [CrossRef]
26. Planet Team. Planet Application Program Interface. In *Space for Life on Earth*; Planet Labs: San Francisco, CA, USA, 2017. Available online: https://api.planet.com (accessed on 15 May 2025).
27. HungaroMet Ltd. Available online: https://odp.met.hu/climate/observations_hungary/monthly/historical/ (accessed on 2 May 2025).
28. Gitelson, A.; Merzlyak, M.N. Spectral reflectance changes associated with autumn senescence of *Aesculus hippocastanum* L. and *Acer platanoides* L. leaves. Spectral features and relation to chlorophyll estimation. *J. Plant Physiol.* **1994**, *143*, 286–292. [CrossRef]
29. Planet Explorer. Available online: https://www.planet.com/explorer/ (accessed on 11 July 2025).
30. QGIS Development Team: QGIS Geographic Information System. Open Source Geospatial Foundation Project. Available online: https://qgis.org (accessed on 30 March 2025).
31. Python Software Foundation. *Python Programming Language*, version 3.x; Python Software Foundation: Beaverton, OR, USA, 2023. Available online: https://www.python.org (accessed on 30 March 2025).
32. Ábri, T.; Borovics, A.; Csajbók, J.; Kovács, E.; Koltay, A.; Keserű, Z.; Rédei, K. Differences in the growth and the ecophysiology of newly bred, drought-tolerant black locust clones. *Forests* **2023**, *14*, 1802. [CrossRef]
33. Kollár, T.; Rédei, K. *Parametrikus Fatermési Táblák*; Soproni Egyetemi Kiadó: Sopron, Hungary, 2025; pp. 271–299. [CrossRef]
34. Peng, Y.; Zeng, A.; Zhu, T.; Fang, S.; Gong, Y.; Tao, Y.; Liu, K. Using remotely sensed spectral reflectance to indicate leaf photosynthetic efficiency derived from active fluorescence measurements. *J. Appl. Remote Sens.* **2017**, *11*, 026034. [CrossRef]
35. Yu, L.; Luo, X.; Croft, H.; Rogers, C.A.; Chen, J.M. Seasonal variation in the relationship between leaf chlorophyll content and photosynthetic capacity. *Plant Cell Environ.* **2024**, *47*, 3953–3965. [CrossRef]
36. Ábri, T.; Gaganetz, D.Z.; Csajbók, J. Light response curve analysis of juvenile black locust clones: A case study from eastern Hungary. *J. For. Sci.* **2024**, *70*, 202–207. [CrossRef]
37. Wang, J.J.; Hu, C.X.; Bai, J.; Gong, C.M. Carbon sequestration of mature black locust stands on the Loess Plateau, China. *Plant Soil Environ.* **2015**, *61*, 116–121. [CrossRef]
38. Chinembiri, T.S.; Mutanga, O.; Dube, T. Landsat-8 and Sentinel-2 based prediction of forest plantation C stock using spatially varying coefficient Bayesian hierarchical models. *Remote Sens.* **2022**, *14*, 5676. [CrossRef]

39. Ma, T.; Hu, Y.; Wang, J.; Beckline, M.; Pang, D.; Chen, L.; Ni, X.; Li, X. A novel vegetation index approach using Sentinel-2 data and random forest algorithm for estimating forest stock volume in the Helan Mountains, Ningxia, China. *Remote Sens.* **2023**, *15*, 1853. [CrossRef]
40. Çinar, T.; Uslu, A.; Aydin, A. Monitoring the rehabilitation process of the windthrow area using UAS images and performance comparison of Sentinel-2A based different vegetation indexes. *Earth Sci. Inform.* **2025**, *18*, 199. [CrossRef]
41. Acharki, S. PlanetScope contributions compared to Sentinel-2, and Landsat-8 for LULC mapping. *Remote Sens. Appl. Soc. Environ.* **2022**, *27*, 100774. [CrossRef]
42. Moon, M.; Richardson, A.D.; Friedl, M.A. Multiscale assessment of land surface phenology from harmonized Landsat 8 and Sentinel-2, PlanetScope, and PhenoCam imagery. *Remote Sens. Environ.* **2021**, *266*, 112716. [CrossRef]
43. Ecke, S.; Dempewolf, J.; Frey, J.; Schwaller, A.; Endres, E.; Klemmt, H.-J.; Tiede, D.; Seifert, T. UAV-based forest health monitoring: A systematic review. *Remote Sens.* **2022**, *14*, 3205. [CrossRef]
44. FAO. *The State of the World's Forests 2024—Forest-Sector Innovations Towards a More Sustainable Future*; FAO: Rome, Italy, 2024. [CrossRef]
45. Sniezko, R.A.; Koch, J.; Liu, J.; Romero-Severson, J. Will genomic information facilitate forest tree breeding for disease and pest resistance? *Forests* **2023**, *14*, 2382. [CrossRef]
46. Sestras, A.F.; Sălăgean, T.; Roman, A.M.; Morar, I.M.; Dan, C.; Truta, A.M.; Sestras, R.E.; Dudescu, M.C.; Spalevic, V.; Kader, S.; et al. Growth and resistance to mechanical stress in the young phase of black locust (*Robinia pseudoacacia* L.) trees based on geographical provenances. *J. Environ. Manag.* **2025**, *384*, 125465. [CrossRef] [PubMed]
47. Budau, R.; Agud, E.M.; Laslo, V.; Timofte, A.I.; Bei, M.F. Genetic Diversity of *Robinia pseudoacacia* L. populations from North-Western Romania revealed by ISSR Markers. *Forests* **2025**, *16*, 1795. [CrossRef]